Available online at www.sciencedirect.com
SCIENCE DIRECT®
Journal of Nuclear Materials 329–333 (2004) 218–222
journal of nuclear materials
www.elsevier.com/locate/jnucmat

Experimental studies on the neutron emission spectrum and activation cross-section for 40 MeV deuterons in IFMIF accelerator structural elements

M. Hagiwara *, T. Itoga, M. Baba, M.S. Uddin, N. Hirabayashi, T. Oishi, T. Yamauchi

Cyclotron and Radioisotope Center, Tohoku University, Aramaki, Aoba-ku, Sendai 980-8578, Japan

Abstract

In order to improve the nuclear data required in the safety design of the International Fusion Materials Irradiation Facility (IFMIF), we have measured the neutron emission spectra and the activation cross-sections of the IFMIF accelerator structural elements, C and Al, for 40 MeV deuterons using the Tohoku University AVF cyclotron. Neutron spectra from thick C and Al targets were measured with the time-of-flight method at ten laboratory angles between 0- and 110-deg. using a beam swinger system and a well collimated neutron flight channel. The data were obtained over almost entire energy range of secondary neutrons using a two-detector method. Activation cross-sections were measured by detecting the γ-rays from C and Al targets with a high-pure Ge detector. The stacked target technique was used to obtain the data from 40 MeV down to the threshold energy.

1. Introduction

The International Fusion Materials Irradiation Facility (IFMIF) project has been proposed to establish an accelerator-based D-Li neutron source for high fluence test irradiations of fusion reactor candidate materials [1]. In IFMIF, a high current (250 mA) of the deuteron beam is accelerated to 40 MeV and transported to the liquid lithium target to produce the neutron field that simulates a fusion reactor neutron field.

For the safety design and management of IFMIF, detailed knowledge on the neutron emission spectrum and the activation cross-section is required. The neutron flux and spectral data are indispensable for accurate estimation of the neutron shielding, and the activation cross-section data are essential for the estimation of radioactivity induced in the accelerator components and shielding materials. Although some studies have already been undertaken on these subjects, the data are very scarce and the data accuracy is not good enough at present [2].

To improve the accuracy of the neutron energy-angular distribution data and the predictability of the radioactivity accumulation in IFMIF, we have been conducting a series of experiments on the neutron emission spectrum of the (d,xn) reaction and the activation cross-section and radioactivity induced in the accelerator components using the AVF cyclotron at the Tohoku University Cyclotron and Radioisotope Center (CYRIC). So far, we have obtained data on lithium targets for 25 and 40 MeV deuterons [3,4].

This paper presents the experiments on: (1) neutron emission spectra from thick aluminum and carbon, and (2) activation cross-sections of the $^{nat}C(d,x)^{7}Be$, $^{27}Al(d,x)^{7}Be$, $^{27}Al(d,x)^{24}Na$ and $^{27}Al(d,x)^{22}Na$ reactions. These data are required for shielding design and radioactivity estimation because these elements are one of the main accelerator components, especially as a beam dump and in the beam tube. The neutron spectra were

* Corresponding author. Tel.: +81-22 217 7806; fax: +81-22 217 7809.
E-mail address: hagi@cyric.tohoku.ac.jp (M. Hagiwara).

0022-3115/$ - see front matter © 2004 Elsevier B.V. All rights reserved.
doi:10.1016/j.jnucmat.2004.04.026

measured at ten laboratory angles between 0° and 110°. The stacked target technique was applied to obtain the activation cross-section from 40 MeV down to the threshold energy.

The experimental results are compared with other experimental data and calculations.

2. Experimental apparatus

The experiments were carried out using the AVF cyclotron at the Tohoku University CYRIC. The experimental apparatus shown in Fig. 1 is almost the same as one employed in the previous measurements with 25 MeV deuterons [3,4]. A deuteron beam accelerated to 40 MeV by the cyclotron was transported to the No. 5 target room which was equipped with a neutron flight channel and a beam-swinger system that enabled angular distribution measurements without changing the detector setup [5]. The frequency of the deuteron beam was reduced to 2.3 MHz with a beam chopper to avoid a frame-overlap in time-of-flight (TOF) measurements.

The thick aluminum and carbon targets were set on a remotely-controllable target changer together with a beam viewer of a ZnS scintillation sheet. The support frame was isolated from ground to read a beam charge induced on the thick target. To measure the number of incident particles accurately, a copper mesh biased to −500 V was installed around the target changer to suppress secondary electrons sputtered from the targets.

Neutrons emitted from the targets were detected by NE213 scintillation detectors, 14 cm-diam × 10 cm-thick and 5 cm-diam × 5 cm-thick, through the 1.5 m-thick concrete–iron collimator which reduced the background events due to neutron scattering and γ-rays from activated components around targets and the beam dump. We adopted a two-detector method to obtain the data over almost the entire energy range of secondary neutrons [4,6]. The larger and smaller detectors were placed around 11.0 and 3.45 m from the targets, respectively. In the measurements with the longer flight path, the NE213 scintillation detector was coupled with a Hamamastu R1250 photo-multiplier and a tube base specially designed for high energy neutrons [7] to measure emitted neutrons for the whole energy region with high energy resolution. The shorter flight path was adopted to measure the low energy part of the neutron spectra without the frame-overlap with high gain. The long and short path measurements covered 5.0–55 MeV and 0.6–30 MeV regions, respectively, of secondary neutron energy range. Using this technique, we obtained the data over almost the entire energy range of secondary neutrons with sufficient energy resolution and good signal-to-noise ratio.

The measurements of the neutron spectra were conducted at 10 laboratory angles (0°, 10°, 15°, 20°, 30°, 45°, 60°, 75°, 90° and 110°) with the beam swinger system. In each measurement, the TOF, pulse-shape-discrimination (PSD) and pulse-height data were collected event by event as three parameter list data for off-line analysis [3,4,6].

3. Target dimensions

The stacked targets were prepared to measure not only thick target neutron spectra but also the

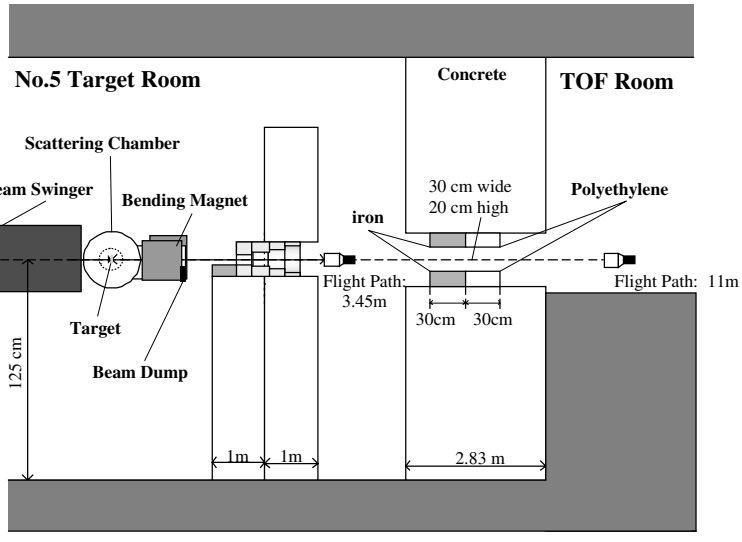

Fig. 1. The layout of the experimental setup at the No. 5 target room in CYRIC.

cross-section of (d,*x*) reactions for aluminum and carbon. The stacked targets consist of thirty elemental aluminum (purity: 99.2%) foils and carbon (purity: 99.8%) foils of approximately 30 mm × 30 mm × 200 μm thick. The total thickness (6 mm) is greater than the range calculated with the SRIM code [8] (5.4 mm in carbon and 4.2 mm in aluminum for 40 MeV deuteron) and enough to stop the incident beam.

4. Experimental procedures

At first, the neutron measurements were performed for 0–110° laboratory angles. During the irradiation, the beam current on the targets was continuously recorded using a mullti-channel scaler (MCS) for normalization of the neutron TOF spectra and for the later activation measurements of the stacked targets. The beam current on the targets was around 5 nA and its pulse width was 2–3 ns in FWHM.

After the irradiation, the activities of ^{7}Be, ^{24}Na and ^{22}Na accumulated in each stacked targets were measured by detecting 477, 1369, and 1275 keV γ-rays, respectively, 18.9 or 5 cm distance from the detector with a high-pure Ge detector (EURICIS MESURESE GPC50-195-R) and a multi-channel analyzer. The dead times during the γ-ray counting were less than 3%.

5. Data analysis

5.1. Neutron spectra

Neutron TOF spectra were obtained by gating the neutron events with a pulse-height bias on two-dimensional pulse height vs. PSD graphical plots and by removing random background events to eliminate γ-ray events. The TOF spectra were converted into neutron energy spectra according to the Lorentz conversion [3,4,6].

The energy spectra were divided by the solid angle of the experimental arrangements, an integrated charge of the incident beam for normalization and the detection efficiency calculated by the Monte Carlo code SCINFUL-R [9]. Finally, the data were corrected for the attenuation in the air and the wall of a vacuum chamber using the total cross-section data of LA150 [10].

5.2. Activation cross-section

The activation cross-section was determined from the peak counts of the γ-ray spectra and the number of incident particles with data corrections for the decay, the peak efficiency of the Ge detector, the self-absorption effect in the samples and the beam current fluctuation during irradiation [3]. The efficiency curves were determined experimentally with standard γ-ray sources. They were corrected for the effect of the self-absorption and the sample size (beam size) using the EGS4 code [11].

The data were corrected for the energy degradation and the attenuation of projectiles through the targets. The incident energy of each stacked foil was estimated by the SRIM code [8]. The number of projectile deuterons was corrected for the attenuation using the total cross-section calculated by Shen's formula [12].

6. Results and discussion

6.1. Neutron spectra

For 40 MeV deuteron, the present results for the ^{nat}C(d,*x*n) and ^{27}Al(d,*x*n) neutron spectra at ten laboratory angles are shown in Figs. 2 and 3, respectively. The data clarified secondary neutron production spectra for the whole energy range. The lower energy limit is approximately 0.7 MeV. The error bars of the spectra represent mainly the statistical errors. The 0–15° spectra show a main peak region centered around 15 MeV, similar to the case of ^{nat}Li(d,*x*n) reaction [13] which is the main neutron source in IFMIF. The shape of the ^{nat}C(d,*x*n) neutron spectra is very similar to the data by Meulders et al. [14] and Radivojevic et al. [15] for 33 and

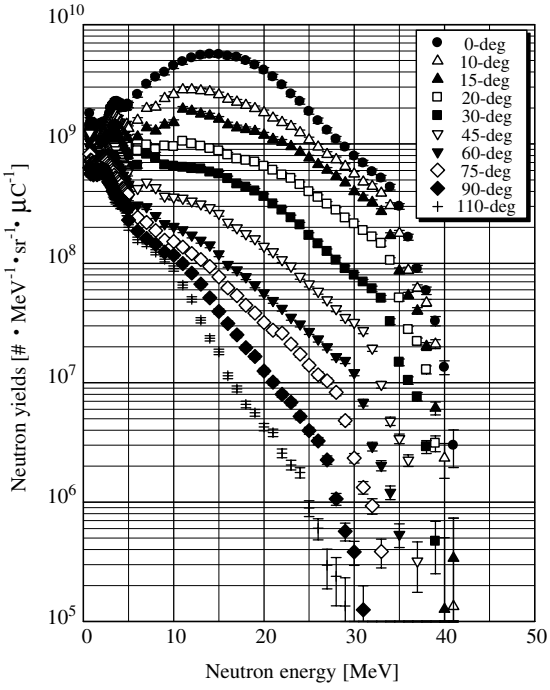

Fig. 2. Neutron energy spectra from a thick carbon target bombarded by 40 MeV deuterons at 10 laboratory angles.

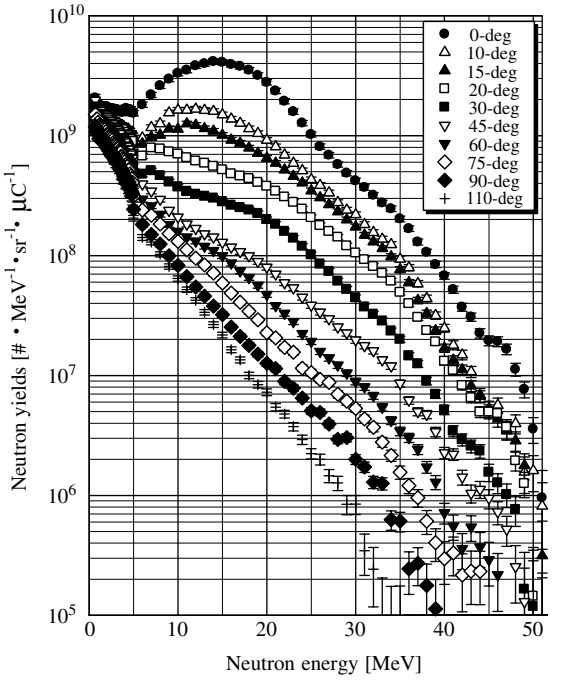

Fig. 3. Neutron energy spectra from a thick aluminum target bombarded by 40 MeV deuterons at ten laboratory angles.

50 MeV deuterons. Generally, these spectra have very strong angular dependence. It can be concluded that the neutrons are produced by similar reaction mechanisms on the main neutron peak region.

The ^{27}Al(d,*x*n) spectra extend up to approximately 50 MeV though the ^{nat}C(d,*x*n) spectra are limited to around incident energy of 40 MeV. This is consistent with the reaction Q-value of 9.36 and −0.28 MeV for the ^{27}Al(d,n) reaction and ^{12}C(d,n) reaction, respectively.

6.2. Activation cross-section

The cross-sections obtained for the ^{nat}C(d,*x*)^{7}Be, ^{27}Al(d,*x*)^{7}Be, ^{27}Al(d,*x*)^{24}Na and ^{27}Al(d,*x*)^{22}Na reactions are compared with other experimental data [16,17] with the evaluated data by the IAEA group [18] and calculations by a recent code PHITS [19]. Fig. 4 shows the comparison for the ^{27}Al(d,*x*)^{24}Na reaction. Though the present data was generally consistent with other experimental data and the evaluated data, they are higher than other data by 10–20%. The PHITS results are similar to the experimental data in shape, but they are much lower in magnitude. The data for the ^{27}Al(d,*x*)^{22}Na reaction are consistent with each other except the PHITS results as shown in Fig. 5. The similar fact is observed for the ^{27}Al(d,*x*)^{7}Be reaction as shown in Fig. 6, though there are no evaluated data. For the

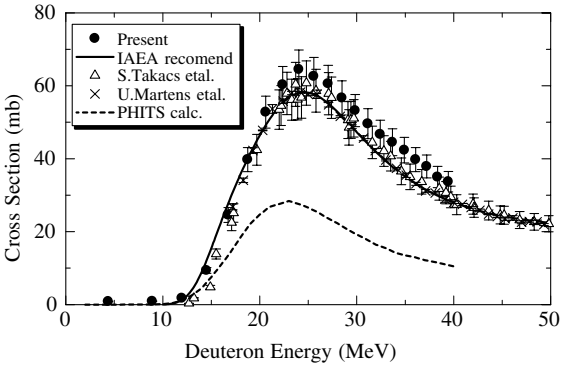

Fig. 4. Comparison of ^{27}Al(d,*x*)^{24}Na reaction cross-sections.

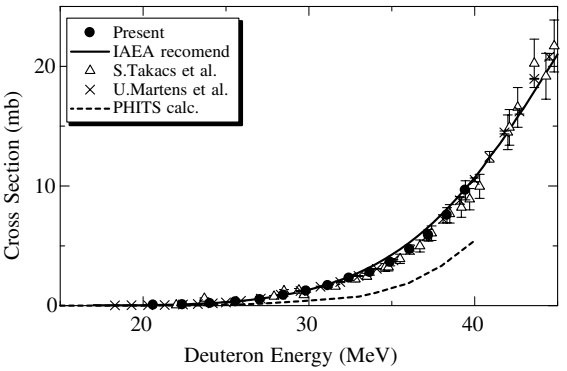

Fig. 5. Comparison of ^{27}Al(d,*x*)^{22}Na reaction cross-sections.

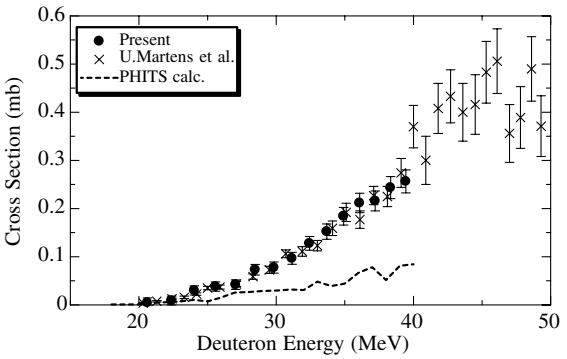

Fig. 6. Comparison of ^{27}Al(d,*x*)^{7}Be reaction cross-sections.

^{nat}C(d,*x*)^{7}Be reaction, the PHITS underestimated the present data as shown in Fig. 7; for this case no other data available. To estimate radioactivity induced by deuterons with PHITS, improvements will be required for cross-section calculation models.

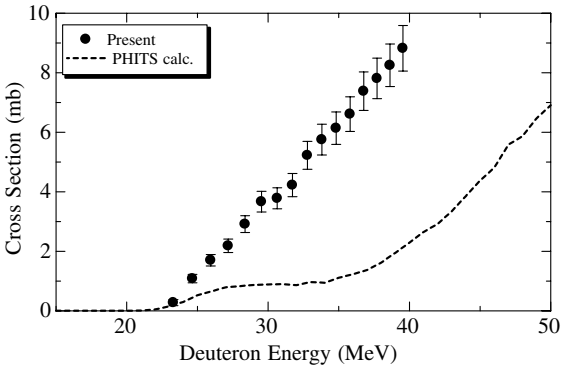

Fig. 7. Comparison of $^{nat}C(d,x)^{7}Be$ reaction cross-sections.

7. Summary

This paper described the experiments of: (1) neutron energy-angular distribution from the C; Al(d,*x*n) reactions and (2) cross-sections of the $^{nat}C(d,x)^{7}Be$, $^{27}Al(d,x)^{7}Be$, $^{27}Al(d,x)^{24}Na$ and $^{27}Al(d,x)^{22}Na$ reaction performed using 40 MeV deuterons at Tohoku University CYRIC. In the neutron measurement, the spectra data for 10 laboratory angles between 0° and 110°. were measured over almost the entire energy range from the maximum energy down to 0.7 MeV. These experimental results will be used as the basic data to check the accuracy of the Monte Carlo simulation and for the shielding design of a medium energy accelerator facility such as IFMIF.

The experimental activation cross-section data were obtained for aluminum and carbon from the threshold energy to 40 MeV. The data were generally consistent with other experimental data and evaluated data. However, the results calculated with PHITS were generally much smaller than experimental values, while the shapes were similar to experimental values. The presented results will be helpful for improvement of the calculation models.

References

[1] IFMIF CDA TEAM, IFMIF Conceptual Design Activity Final Report edited by Marcello Martone, Report 96.11, Enea, Dipartimento Energia, Frascati, 1996.
[2] M.A. Lone et al., Nucl. Instrum. and Meth. 143 (1977) 331.
[3] M. Baba, T. Aoki, M. Hagiwara, et al., J. Nucl. Mater. 307–311 (2002) 1715.
[4] T. Aoki, M. Hagiwara, M. Baba, et al., J. Nucl. Sci. Technol. 41 (4) (2004) 399.
[5] A. Terakawa et al., Nucl. Instrum. and Meth. A 491 (2002) 419.
[6] T. Aoki, M. Baba, S. Yonai, N. Kawata, M. Hagiwara, T. Miura, T. Nakamura, Nucl. Sci. Eng. 146 (2004) 200.
[7] M. Baba, H. Wakabayashi, M. Ishikawa, T. Ito, N. Hirakawa, J. Nucl. Sci. Technol. 27 (7) (1990) 601.
[8] J.F. Ziegler, J.P. Biersack, U. Littmark, The Stopping and Range of Ions in Solids, Pergamon, New York, 1984.
[9] S. Meigo, Nucl. Instrum. and Meth. A 401 (1997) 365.
[10] M.B. Chadwick, P.G. Young, et al., Nucl. Sci. Eng. 131 (1999) 293.
[11] W. Nelson, H. Hirayama, D.W.O. Rogers, 'The EGS4 Code System' SLAC-265, Stanford University, Stanford, CA, 1985.
[12] W.Q. Shen, B. Wang, J. Feng, W.L. Zhan, Y.T. Zhu, E.P. Feng, Nucl. Phys. A 491 (1989) 130.
[13] S.P. Simakov, U. Fisher, U. von Mllendorf, I. Schmuck, A.Yu. Konobeev, Yu.A. Korvin, P. Pereslavtsev, J. Nucl. Mater. 307–311 (2002) 1710.
[14] J.P. Meulders et al., Phys. Med. Biol. 20 (1975) 235.
[15] Z. Radivojevic, A. Honkanen, J. Aysto, V. Lyapin, V. Rubchenya, W.H. Trzaska, D. Vakhtin, G. Walter, Nucl. Instrum. and Meth. B 183 (2001) 212.
[16] S. Takacs, F. Szelecsenyi, F. Tarkanyi, M. Sonck, A. Hermanne, Yu. Shubin, A. Dityuk, M.G. Mustafa, Z. Youxiang, Nucl. Instrum. and Meth. B 174 (2001) 235.
[17] U. Martens, G.W. Schweimer, Z. Phys. 233 (1970) 170.
[18] IAEA, Charged-particle cross section database for medical radioisotope production http://www-nds.iaea.org/medical.
[19] H. Iwase, K. Niita, T. Nakamura, J. Nucl. Sci. Technol. 39 (11) (2002) 1142.